# INVESTIGATION OF FLUID MECHANICS OF SLOTTED AIR-JETS FOR AIR REVERSER APPLICATIONS

by

**E. Lopez and S. Müftü**
**Northeastern University**
**USA**

## ABSTRACT

The fluid mechanics of the air flow, caused by a series of impinging air-jets, in a constant-height, rigid channel is investigated using computational fluid dynamics (CFD). The primary goal of this work is to investigate the effects of the interactions between different air-jets. The model is representative of a cross section of the clearance between a web and an air-reverser. A cross flow is generated by the air trapped in the clearance. Using the CFD package Fluent, the effects of channel-height, spacing between the air-jets, supply pressure for the air-jets and number of jets, on the flow characteristics is investigated. In particular a flow "loss" coefficient, defined as the ratio of the velocity obtained using average velocity of each jet from the CFD analysis to the velocity obtained from the Bernoulli's equation, was shown to vary from air-jet to air-jet. It was found that a lower channel-clearance increases jet interaction, as it forces jets to flow into each other. Larger spacing of the air-jets also increases jet interaction, as cross flow fully develops into lateral flow. Supply pressure was seen to have a small effect. The flow "loss" coefficient behavior was characterized as functions of these variables.

## 1 INTRODUCTION

Multiple impinging jets are used today in a number of industrial applications. These jets can be used for heating and cooling of surfaces, such as drying paper and textiles, cooling electronics and tempering glass. Much work has been done to study the effects of various arrangements on flow behavior and heat transfer in an effort to make these

arrangements more efficient. In a web handling application, such as photographic film or paper manufacturing, the running direction of a continuous web needs to change often. At certain process locations on the web-path, the web can not be supported by rollers to change its direction, as contact could damage the product. Air reversers allow the web to float on a cushion of air, thereby protecting the web. An air reverser is a pressurized hollow drum with holes on the surface to provide the air cushion.

Multiple impinging jets with and without cross-flow closely represents the setup of an air reverser and the flow produced. Most of the research available focuses on heat transfer, as cooling applications is a typical use for these jets. Al-Sanea developed a two dimensional CFD model to study the steady flow and heat transfer characteristics of three types of slot jets impinging on a surface [2]. The types of jets included a free jet, a semi-confined jet and a semi-confined jet in a cross flow. Geometrical parameters such as jet width, distance from surface and surface length were studied as well Reynolds number and crossflow to jet exit mass flow rate ratio. Emphasis was placed on heat transfer, but it was shown that a distance away from the impingement region flow behaves like a wall jet. Cross-flow shifts the impingement point downstream, and flow interaction occurs also downstream.

Yang and Hao studied the fluid flow of three turbulent slot jets while varying parameters such as Reynolds number, clearance and pitch [3]. Their paper describes the flow field into six characteristic regions: the free jet region at the jet exit, the impinging jet region, the wall jet development region, the fountain formation region, the fountain up-wash region and the recirculation region. Flow interaction was seen depend on hole pitch and clearance. Similar observations are made in the present work; despite the lack of externally imposed cross-flow.

Barata et al. experimentally studied two and three turbulent impinging jets through a crossflow by using laser Doppler velocimetry [4]. Their study identified the formation of fountain up-wash and recirculation regions caused by flow interaction. It was noted that the collision of wall jets caused the recirculation regions and interaction is intensified with the addition of another jet. The results suggested that the flow of impinging jets is turbulent in nature.

Saad, Polat and Douglas compared a single impinging jet model to a multiple jet configuration with exhaust outlet between jets [5]. Interaction between jets was shown to have a dependence on the spacing between jets. Interaction was defined as the deviations from the single jet model. Pressure profiles showed that defining a volume cell as the spacing between jets and clearance is adequate. The critical $S/H$ ratio of jet spacing $S$ to channel clearance $H$ was found to range from 0.75 to 1. Jets behave as a single jet above this value. It should be keept in mind that this configuration had exhaust ports on the top wall. Authors also found that the jet size has a small affect on the extent of the stagnation region.

Kim and Benson investigated the interactions between a row of confined impinging jets and a perpendicular cross-flow [6]. They showed that a vortex develops behind the jet and that this causes an obstruction to the cross-flow. They also showed that using either constant pressure or velocity is not valid to model the flow at the jet exit. The cross flow can effect the flow down into the jet and across the jet.

Jet interaction was further examined by Seyedein et al. who analyzed a turbulent flow field and impingement heat transfer due to three and five heated slotted jets, discharging normally into a confined channel [7]. Effects of jet-to-jet spacing and jet-to impingement surface spacing were investigated. They found that cross-flow develops by the spent-flow form the upstream nozzles. Recirculation regions decrease in size downstream due to the increase in cross-flow. Increasing clearance causes the size of the

recirculation regions to increase. Pressure along the impingement surface drops away from the jets, but increases slightly as it approaches the neighboring jet. Jet interaction due to the upstream holes was shown to decrease. The effect of Reynolds number was seen to have little effect on the flow pattern.

The effect of an inclined confinement surface was investigated by Yang and Shyu [15]. It was found that the maximum local Nusselt-number and maximum pressure on the impinging surface move downstream, with increasing inclination angle $\theta$. Inclination angle also had a significant effect on the size of the recirculation regions.

Lewis [1] developed the governing equations for the two dimensional fluid flow in the clearance between the air reverser and web. These equations are derived in the plane of the web by averaging the flow variables through the thickness direction of the web-reverser clearance. The density of the holes on the surface of the reverser was assumed high enough to consider the hole distribution as being averaged over the reverser surface. The frictional losses at the discharge of the holes were lumped into a discharge loss coefficient. In this work the fluid mechanics in the web-reverser clearance is modeled through the thickness direction of the reverser using commercially available CFD program Fluent. Primarily, the interaction between the jets injecting air into the reverser-web interface is investigated. The study is two-dimensional. Hence, the jets become slotted jets in this work.

## 2 AIR REVERSER MODEL

### 2.1 Governing Equations

The equations of motion for the fluid flow in the clearance of a web and an air reverser are derived by averaging conservation of mass and momentum equations over the clearance between reverser and the web [1]. Figure 1 shows a cross-section of the web-reverser clearance. In this figure the $z$-direction is the aligned with the (vertical) clearance. The airflow is assumed to be 2D in the plane of the web (i.e., $x$-$y$-plane). In this figure the $y$-direction, which is not shown, is oriented to form a right handed, orthogonal coordinate system. The following assumptions are made about the flow:

- Clearance between air reverser and web is small enough to consider the flow two dimensional in the plane of the reverser surface.
- Hole spacing is small enough to consider air supply a uniform and distributed source.
- Flow is incompressible and viscous forces are negligible.

Then, the governing equations for the $x$-$y$ plane become:

$$\frac{\partial h}{\partial t}+\frac{\partial hu}{\partial x}+\frac{\partial hv}{\partial y}=\alpha U \tag{1}$$

$$\rho\frac{\partial u}{\partial t}+\rho u\frac{\partial u}{\partial x}+\rho v\frac{\partial u}{\partial y}+\frac{\partial p}{\partial x}=-\alpha\rho U\frac{u}{h} \tag{2a}$$

$$\rho\frac{\partial v}{\partial t}+\rho u\frac{\partial v}{\partial x}+\rho v\frac{\partial v}{\partial y}+\frac{\partial p}{\partial y}=-\alpha\rho U\frac{v}{h} \tag{2b}$$

$$U=\kappa(2(p_a-p)/\rho)^{\frac{1}{2}} \tag{3}$$

where $\alpha$ is the hole density, $\kappa$ is the discharge coefficient, $\rho$ is the density of air, $U$ is the hole velocity, $h$ is the clearance between the web and reverser in the z-direction, $p$ is local pressure and $p_o$ is the supply pressure. The flow components in the $x$- and $y$-directions are $u$ and $v$.

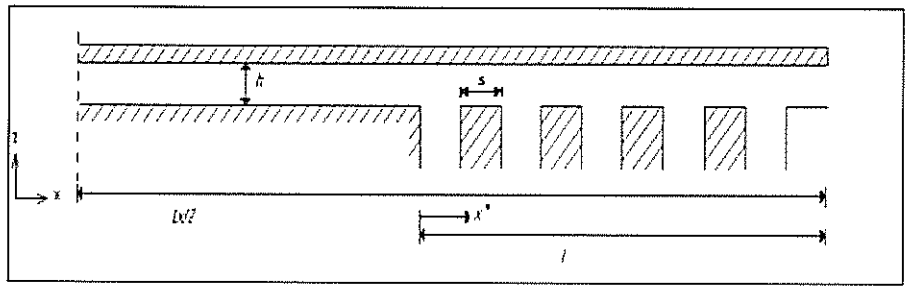


Figure 1 – One half of the 1D problem

Equation (1) is the mass conservation equation with an added source on the right hand side. Since it is assumed that air holes are sufficiently close and considered a uniform source, we can represent the source as a product of hole density and hole velocity. Hole density ($\alpha$) is the ratio of total cross sectional area of the hole to the total surface area. Equations (2a) and (2b) represent the momentum flux through the holes, where $u$ and $v$ are the local $x$ and $y$ velocities of the flow, respectively. These equations also depend on the local hole velocity ($U$) and hole density ($\alpha$). Equation (3) provides an expression for the hole velocity ($U$), which is usually not constant and varies from hole to hole. Hole velocity is a function of pressure drop across the hole. The losses due to friction, are approximated by the discharge coefficient $\kappa$, which ranges from 0 to 1.

## 2.2 One Dimensional Solution

Müftü et al. described a closed form solution to the one dimensional (1D) problem (Fig 1), where the flow velocity $u$ and air pressure $p$ in the hole region ($0 \le x' \le l$) are predicted by [1]:

$$u = U_o \frac{\sinh(mx'/l)}{\sqrt{2}\cosh(m)} \tag{4}$$

$$p = p_o\left[1-\left(\frac{\cosh(mx'/l)}{\cosh(m)}\right)^2\right] \tag{5}$$

where $l$ is the length of the hole regions, $m = \sqrt{2}\kappa\alpha l/h$ and $U_o = \sqrt{2p_o/\rho}$ [1]. The parameter $m$ represents the ratio of effective hole-area to total exit area at the edge of the web. Average pressure for the 1D solution over the entire web area then becomes [1]:

$$p_{ave} = \left(1-\frac{2l}{L_x}\right)p_1 + \left(\frac{2l}{L_x}\right)\bar{p} \tag{6}$$

where

$$p_1 = p_o\left[1-\frac{1}{\cosh^2(m)}\right] \tag{7}$$

and

$$\overline{p} = \frac{1}{l}\int_0^l p\,dx = p_o\left[1 - \frac{1 + \frac{\sinh(2m)}{2m}}{1 + \cosh(2m)}\right]. \qquad (8)$$

## 3 NUMERICAL MODELLING

In this work, two dimensional solutions in the $x$-$z$ plane were obtained using Fluent (ver.5.5, Lebanon, New Hampshire) software package, in order to investigate the effects of interactions of the air jets. The solution mesh for this problem was generated using the Gambit grid generator (ver.2.04, Lebanon, New Hampshire). Symmetry of the solution domain was utilized. Among the various turbulence models used by Fluent, the one equation Sparlart-Allmaras turbulence model, combined with Simplec algorithm provided the most stable, efficient and consistent results. For all configurations, default values for Sparlart-Allmaras viscosity model constants were used. Under-relaxation constants found in Solution Controls of Fluent were changed to allow for convergence of all configurations. Pressure, momentum and modified turbulent viscosity under-relaxation constants were reduced by a factor of two.

In this work, interactions of four, six, eight, ten and twelve supply holes on the flow characteristics were considered. Due to symmetry a configuration with two supply-holes, has only one hole in the modeled area. Similarly, a case with four holes has two holes, and so on. Figure 2 shows the model for a configuration with ten supply holes. In this work, hole-pitch (S) values of 3, 6 and 24 mm were considered. A hole diameter of 3 mm was used for all configurations. Hole density ($\alpha$) is changed by adding more holes and extending the length of the hole area, $l$.

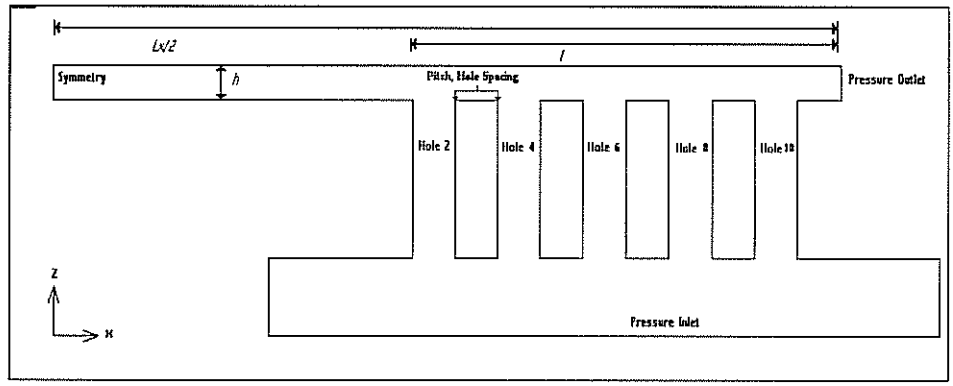


Figure 2- An example of the 10-hole geometry configuration modeled in Fluent.

### 3.1 Numerical Convergence of the Model

Before any data could be collected, it was necessary to test the solution method. This required studies in mesh size, boundary conditions and residual limits. In order to examine the effect of the size of the solution mesh a convergence study was conducted. The convergence tests were performed using a configuration where a single hole is centered in the solution domain, with $h$ = 1 mm gap height, under $p_o$ = 600 Pa supply

pressure. Convergence of the pressure along the top wall was monitored as a function of mesh size. A uniform spatial mesh $\Delta x = \Delta y$ was used in the study. Tests were performed on $\Delta x = 0.25$, 0.2, 0.15, 0.1 and 0.05 mm orthogonal meshes. Figure 3 shows the effect of solution mesh size on the pressure value along the top wall. It is seen that the variation between the $\Delta x = 0.1$ and $\Delta x = 0.05$ mm was less than 1% of the average pressure. The 0.1 mm mesh provides sufficient resolution and half the computation time as compared to 0.05 mm mesh. Therefore, for the rest of this work $\Delta x = \Delta y = 0.1$ mm was used.

Residual limits for $u$ and $v$, fluid velocities in $x$- and $y$-directions, respectively and mass conservation, (found in Solution Controls of Fluent) were set to $10^{-7}$ for each variable, in order to allow for proper convergence. Deviations between solutions taken to different residual limits are on the order of magnitude of $10^{-2}$. These fluctuations cause problems when velocities and pressure are same order of magnitude with these fluctuations. More is discussed about this in loss coefficient section.

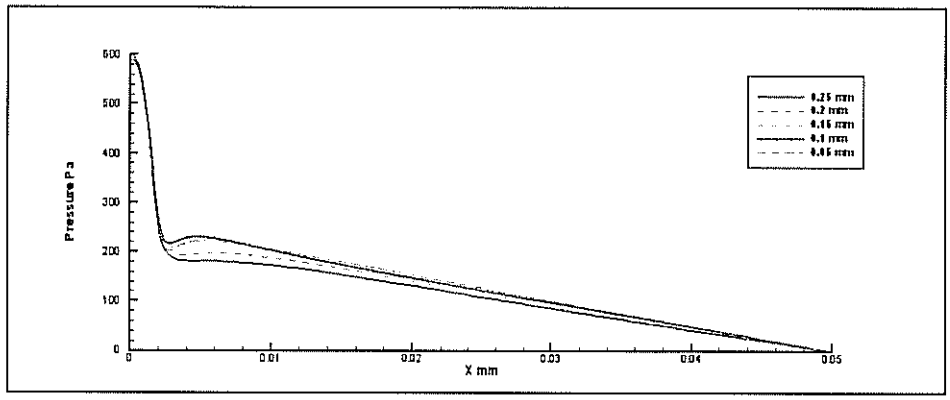


Figure 3 - Pressure profiles from mesh test

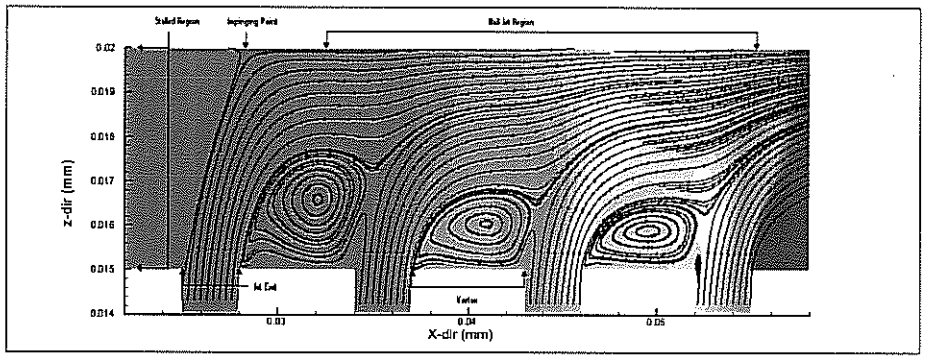


Figure 4 - Example of flow characteristics for $p_o = 600\,Pa$, $h$ = 5 mm.

## 4. GENERAL CHARACTERISTICS OF THE FLOW

A typical steady state solution for an eight hole configuration, with $h$ = 5 mm is shown in Figure 4. In this figure, the air pressure magnitude in the clearance is indicated by the colored contours, and the flow direction is indicated by the stream lines This and other results indicate that the flow in the channel can be separated into five distinct regions, also defined in reference [3].

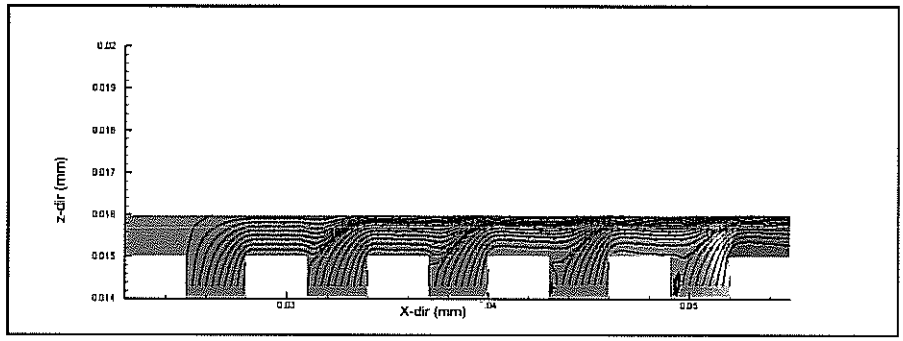


Figure 5a - Ten holes at 1 mm height, no vortices.

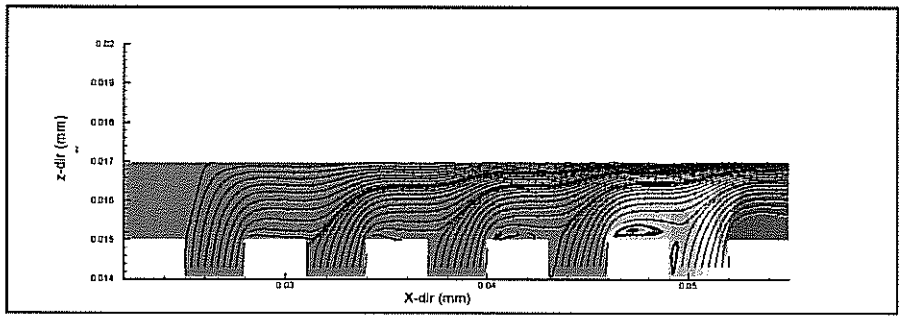


Figure 5b - Ten holes at 2 mm height, vortices form.

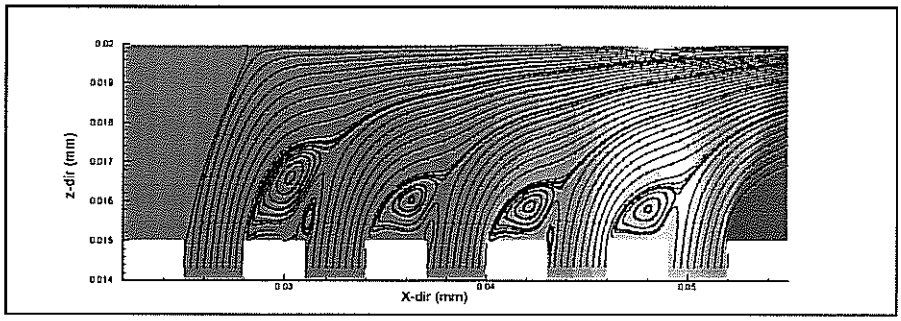


Figure 5c - Ten holes at 5 mm height, greatest.

The *impinging jet region* is the vicinity of the stagnation point of the jet on the top wall. This work showed that this stagnation point has slight dependence on gap height. As gap height increases, the stagnation point moves toward flow exit. Following this region the flow typically turns toward the exit region and develops a "jet" along the top wall. The *wall jet region* is the combination of flows exiting the hole region along the top wall. Wall jet development depends strongly on the hole spacing and the vortex size. Greater hole-spacing leads to a more defined wall jet between the holes. *Stalled flow region* lies in the main central area between the left and right hole regions. In this region the flow is negligibly slow. Finally, *vortices* develop in the area trapped by neighboring jets and the wall jet region. Typically, the number of vortices depends on the number of holes. Location, presence and intensity of these characteristic regions depend on number of holes, clearance height and spacing between holes.

Effect of clearance height $h$ on the vortex formation is shown in Figure 5. This figure shows that the vortex size increases with increasing clearance values. For the clearance height of 1mm, shown in Figure 5a, no noticeable vortices can be seen. Formation of the vortices begins at the 2 mm height and intensity is strongest at the hole nearest the exit shown in Figure 5b. As height is increased the center vortices gain in size and become the most dominant of the vortices in the configuration, as shown in Figure 5c for $h$ = 5mm.

Greater hole pitch allows the vortices to reach a maximum in size, where the wall jet extends to the confining surface. The smallest hole pitch (3 mm) allows vortices to become compacted and even impinge on the nearby hole as pressure drops near the exit, shown in Figure 5c.

The vertical component ($w$) of the air velocity is investigated in Figure 6. This figure is instructive in investigating how much air is moving into the clearance from the holes (jets). In general this figure shows that the $w$-component of the air velocity increases near the exit region, with an accompanying drop in air pressure (not shown in Figure 6). In particular, Figure 6a shows a twelve–hole configuration where the only significant vertical flow occurs on the outermost two holes. The air velocity of the inner most hole is greatly affected by the number of holes and the clearance height. For the low height of $h$ = 2 mm, shown in Figure 6a, the innermost holes have extremely low flow rates as compared to the outer holes due to pressure build-up in the center.. Increasing number of holes does not necessarily increase flow rate into the gap, because at a certain gap height, only a number the outer most holes are effective. This can be seen in Figures 6b and 6c, as the velocity contours for both the eight and twelve hole configurations at same gap height of 5 mm are nearly identical. Due to conservation of mass, increasing number of holes does not always increase flow rate, but increasing gap height allows more air to enter the interface.

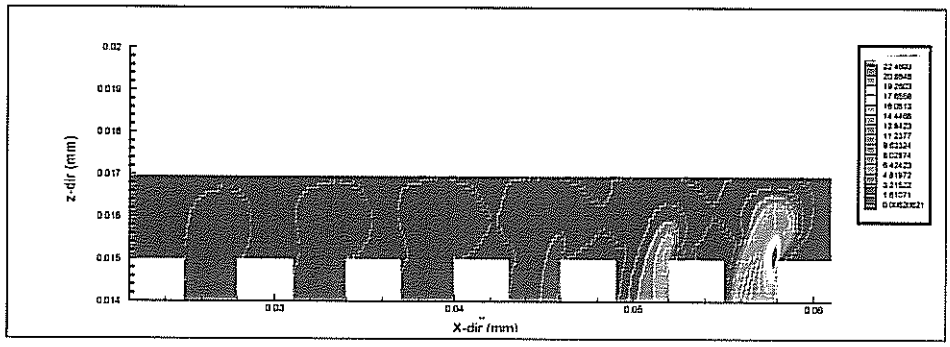


Figure 6a - Velocity component in the $z$-direction for twelve hole 2 mm gap height.

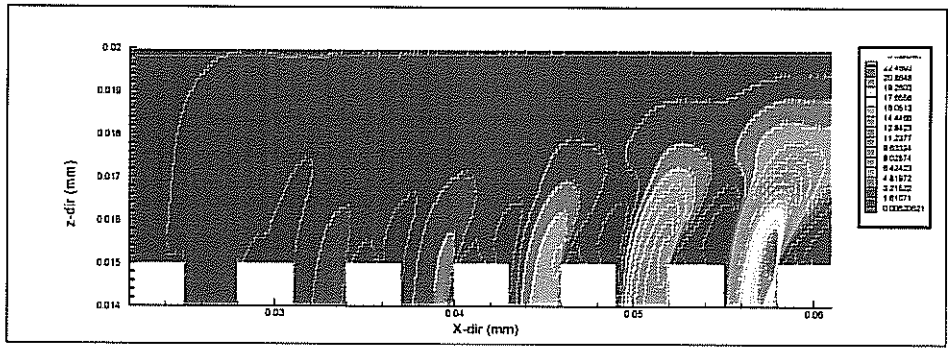


Figure 6b - Velocity component in the $z$-direction for twelve hole 5 mm gap height.

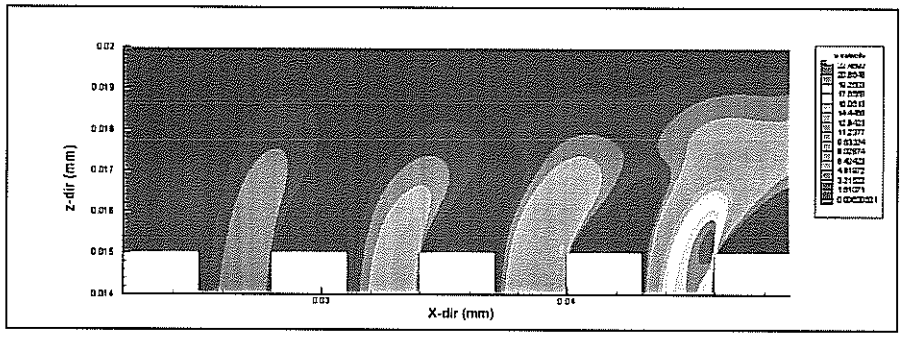


Figure 6c-Velocity component in the $z$-direction for eight hole 5 mm gap height.

## 5. AIR PRESSURE CHARACTERISTICS

The primary interest in air reversers is due to their ability to float tensioned webs. For this reason, it is critical to determine the characteristics of the air pressure profiles along the top wall. Equations (4) and (5), indicate that pressure decreases as the clearance height increases. The effect of hole pitch $s$, and clearance height $h$ on the pressure profile on the top wall of the channel is investigated in Figure 7. The hole-pitch

values of $s$ = 3, 6 and 244 mm are shown in Figures 7a – 7c, respectively, and each figure also shows the clearance height values of $h$ = 1, 3 and 5 mm.

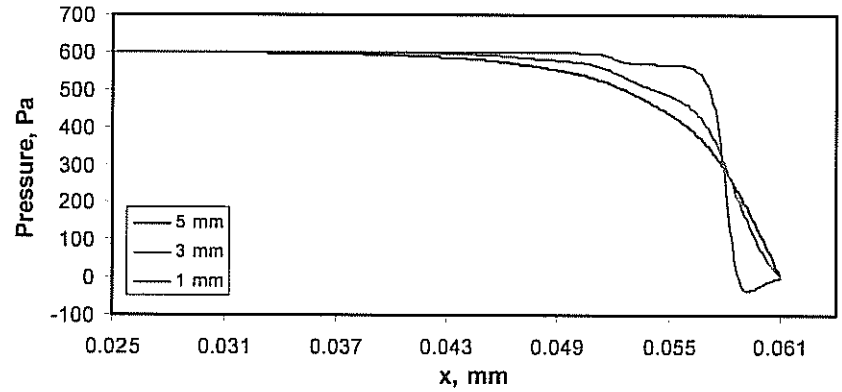


Figure 7a - Pressure profiles at the top for twelve hole at varying clearance, with hole pitch 3 mm.

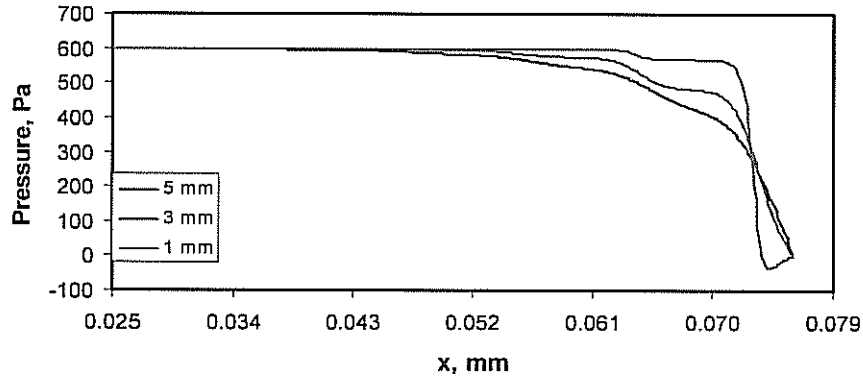


Figure 7b - Pressure profiles at the top for twelve hole at varying clearance, with hole pitch of 6mm.

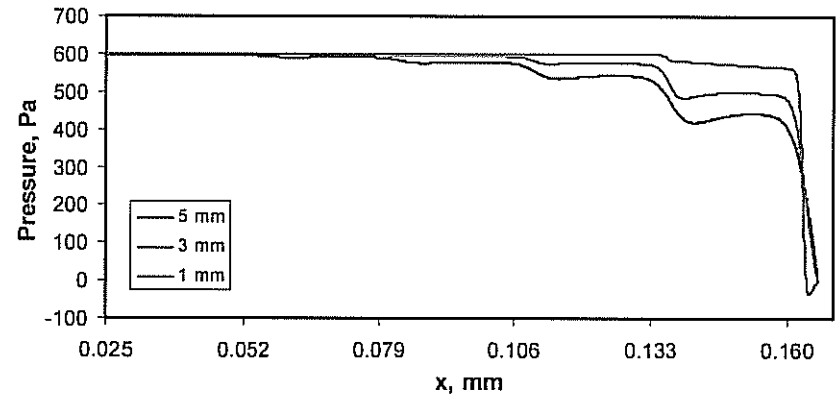


Figure 7c - Pressure profiles along the top for twelve hole at varying clearance, with hole pitch 24 mm.

This figure shows that the configuration with smaller pitch maintains a higher average pressure for greater clearance height values. Smaller pitch also creates a smoother hole-to-hole pressure transition . Increasing the number of holes also increases the configurations ability to sustain a higher pressure for increasing gap heights.

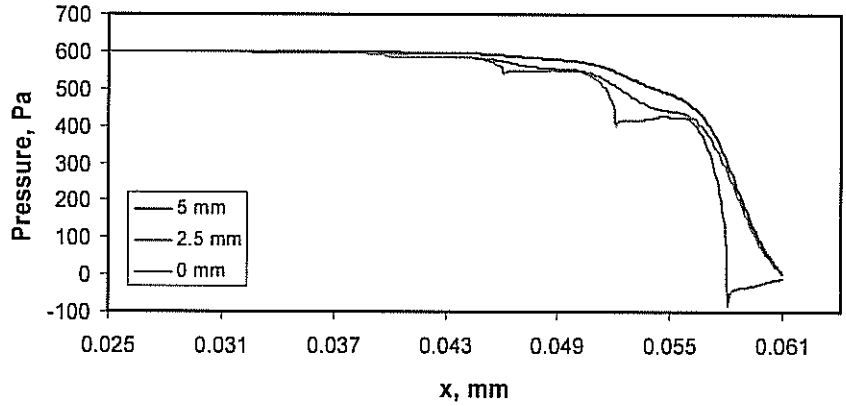


Figure 8a - Pressure profiles at heights 0, 2.5 and 5 mm for a total gap height of 5 mm, calculated for a hole pitch of 3 mm.

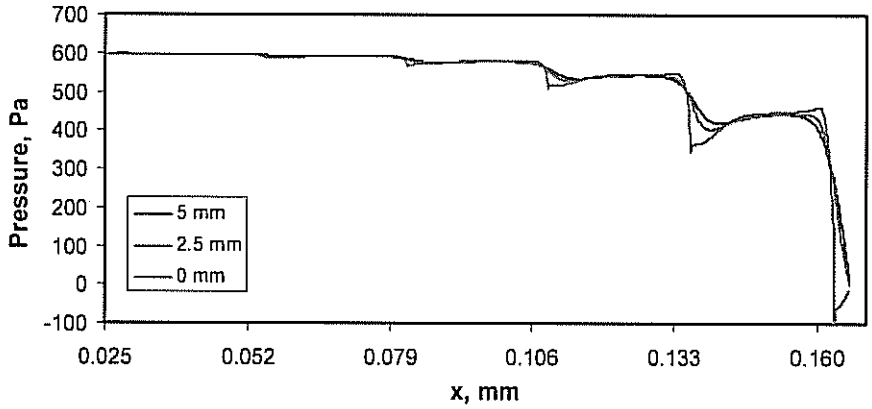


Figure 8b - Pressure profiles at heights 0, 2.5 and 5 mm for a total gap height of 5 mm, calculated for a hole pitch of 24 mm.

The uniformity of air pressure in the vertical ($z$-) direction is investigated in Figure 8, for a clearance value of $h$ = 5 mm, at three different cross-sections located at $z$ = 0, 2.5 and 5 mm.

Figure 8a shows the pressure profiles for the case of hole-pitch of $s$ = 3 mm, and Figure 8b shows the same for $s$ = 24 mm. An assumption for the governing equations is clearance between air reverser and web is small enough to consider the flow two dimensional in the plane of the reverser surface and that the pressure is constant through the clearance height. Results show that, air pressure is constant in the central-region between the hole areas, but it starts to change in the hole-region. It was also found that the extent of the uniform pressure depends highly on hole-pitch. Vortices are the primary cause of the pressure non-uniformity.

When hole-pitch is small, as in Figure 8a, pressure is non-uniform, because vortices dominate the entire length between holes. As the hole-pitch increases, pressure can be considered constant outside the immediate area of the vortices, as shown in Figure 8b.

## 6 LOSS COEFFICIENT

The discharge coefficient defined for pipe-flow represents the frictional losses in the fluid due to an obstruction. In a pipe flow, the discharge coefficient is a function of the diameter ratio of the pipe to the obstruction opening, the specific geometry of the obstruction and the Reynolds number [16]. In the channel flow as described in this paper, in addition to these quantities, the losses also depend on the interaction of the side flow with the incoming jet flow. In the present problem, the situation is further complicated by the fact that the amount of side flow depends on the interaction between the holes and the channel geometry. Therefore, it is not surprising to see that a simple vena-contracta does not exist for the flow investigated in this problem. Despite this, a loss coefficient can still be defined. A distinction is made between the loss coefficient $\kappa_L$ defined below, and the discharge coefficient of pipe flow due to the different ways they are calculated.

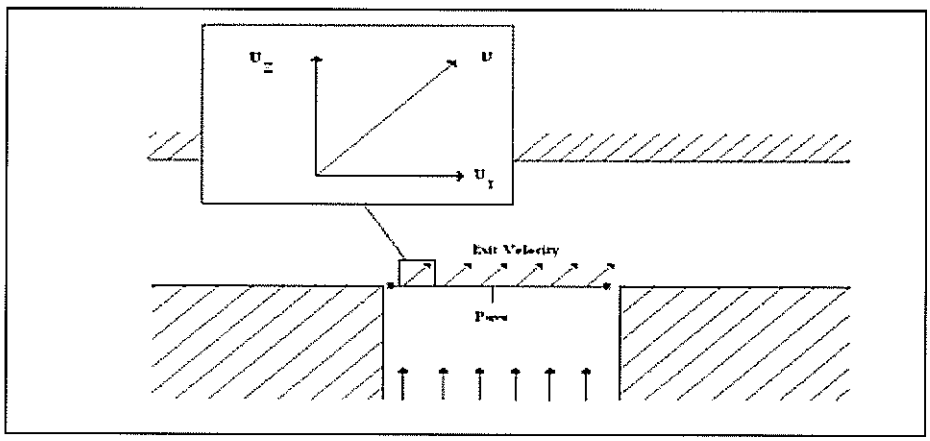

Figure 9 – Definitions of flow components, for calculation of the loss coefficient,

Here the loss coefficient ($\kappa_L$) is defined as the ratio of the average vertical velocity from the numerical solution $w_{ave}$ at the hole-opening, to the ideal hole exit velocity $U_{Ideal}$, based on Bernoulli's equation:

$$\kappa_L = \frac{w_{ave}}{U_{Ideal}} \tag{9}$$

The flow components that enter this calculation are depicted in Figure 9. This parameter is calculated for each hole separately. Here $w_{ave}$ is calculated from the results of the numerical solution, where as $U_{Ideal}$ is given as,

$$U_{Ideal} = \sqrt{\frac{2(p_o - p_{ave})}{\rho}} \quad . \tag{10}$$

where $p_o$ is the supply pressure and $p_{ave}$ is the average pressure along the opening of a hole, as shown in Figure 9.

In this section the effects of various variables, such as clearance height ($h$), hole-pitch (s), hole location, hole depth and supply pressure ($p_0$), on the loss coefficient ($\kappa_L$) of the individual holes are investigated.

## 6.1 Numerical considerations

Due to the nature of the numerical solution, at certain gap heights, the magnitude of the average jet velocities are on the same order of magnitude as the convergence limit. These velocities are kept out of the loss factor calculations. A scheme to determine which holes should be neglected was developed based on the similar behavior of hole velocities for all configurations. We found that, at a 1 mm gap height only the two outer most holes should be considered. At 2 mm gap, the three outermost holes would be acceptable. This continues in a linear fashion, until at 5 mm only the 6 outermost holes are considered, as shown in Table 1. If the present configuration were to only have 5 holes then at 4 mm gap height no holes will be neglected. It was shown above that the innermost holes have the smallest air velocities, therefore, neglecting the loss coefficient calculation for these holes has negligible effect on our goals.

| Gap height (mm) | Outermost holes considered |
|---|---|
| 1 | 2 |
| 2 | 3 |
| 3 | 4 |
| 4 | 5 |
| 5 | 6 |

Table 1 - Scheme for accepting discharge coefficients

## 6.2 Effect of Supply Pressure on $\kappa_L$

In order to test for any correlation between the loss coefficient $\kappa_L$ and supply pressure $p_0$, a twelve-hole configuration with $s$ = 3 mm pitch was subjected to 600, 750 and 900 Pa supply pressures. Loss coefficient values at each hole were calculated as discussed above. It was found that the difference between the loss coefficients calculated for different supply pressures, for these inputs parameters, was insignificant. Due to these small changes a supply pressure of 600 Pa was used in this study.

## 6.3 Effect of Hole Pitch on $\kappa_L$

Cross flow generated by the wall jet is a major factor for the loss coefficient. Hole pitch and wall jet development are found to be related. Figures 10 and 11 show the flow streamlines for the hole pitch values of 3 mm and 24 mm, respectively, for a clearance of $h = 5$ mm. These figures show that the wall jet is allowed to develop and expand through the gap height for higher hole-pitch values. This cross-flow then interacts with the next jet affecting loss coefficient. For the largest pitch, loss coefficients are the lowest

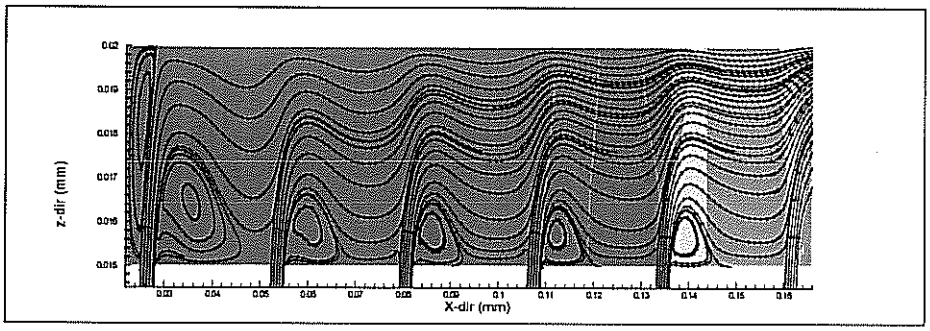


Figure 10 – Streamlines of twelve hole largest hole pitch (24 mm) at 5 mm gap height.

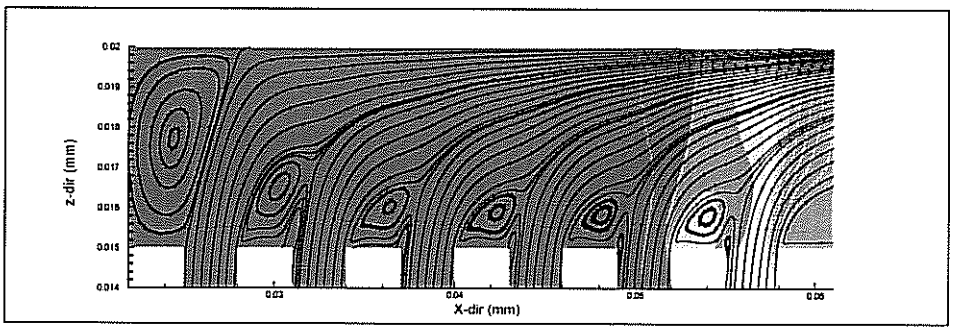


Figure 11 - Streamlines of twelve hole smallest hole pitch (3mm) at 5mm gap height.

because the cross-flow in between holes has the greatest development and has stronger interaction with the following hole. For the smallest pitch, vortices dominate the flow between the holes and actually shield the next hole from the effects of the cross-flow.

Figure 12 shows the loss coefficient values at each hole for a 12-hole configuration, with $h = 5$ m, and three different hole-pitch values of $s = 3$ mm, 6 mm and 24 mm. This figure shows that the loss coefficient values for these configurations is on the order of 0.6 – 0.65. More losses occur for higher whole-pitch values, and there is a slight trend of increasing $\kappa_L$ toward the outer holes. This trend holds for $h = 3$, 4 and 5 mm, where flow out of jets is hampered by pressure buildup, as shown in Figure 10 and 11. At 1 and 2 mm gap heights, the trend reverses and now the largest pitch has the higher loss coefficient. This occurs because the vortices no longer shield the neighboring jets from cross-flow which have is stronger for smaller pitch.

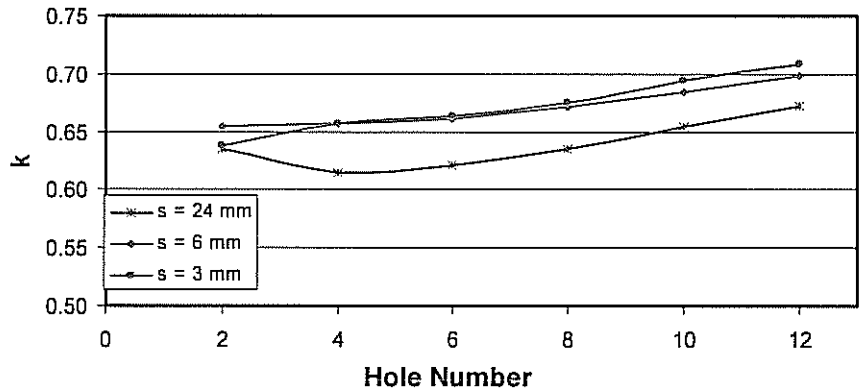

Figure 12 - Loss coefficients of twelve hole 5 mm gap height for varying hole pitch values.

## 6.4 Effect of Number of Holes

The effect of number of holes on the loss coefficient $\kappa_L$ is investigated in Figure 13, where four, six, eight, ten and twelve hole configurations with hole-pitch of $s = 24$ mm and clearance value of $h = 5$ mm is analyzed. This figure shows that increasing number of holes increases the likelihood of interaction between holes, which eventually lowers the loss coefficient. Interestingly, adding more than two to three holes inward (towards symmetry axis) from a given hole has little to no effect on its loss coefficient. For example, comparing a four-hole configuration with a six-hole one it is seen that the loss coefficient of the outermost hole will change on average by 0.02. Comparing six-hole to eight-hole configurations the change is approximately 0.01. The change from eight-hole to ten-hole and ten-hole to twelve-hole is so minimal that the loss coefficient can be considered constant. In particular, Figure 13 allows us to track the decrease of $\kappa_L$ at the outermost two holes (i.e., holes -10 and -12), as more holes are added. This trend holds for all gap heights and all hole pitch values. For all practical purposes limit on hole interaction can be set to three. Meaning once three holes have been established inward from another hole, the loss coefficient will not change.

## 6.5 Effect of Gap Clearance

The factor with the greatest contribution to loss coefficient is gap height and is simplest to understand. Figure 14 shows the hole-to-hole variation of the loss coefficient $\kappa_L$ for a twelve-hole configuration, with 24 mm hole pitch under varying clearance values. In general this figure shows that the losses are less for higher gap clearance values. In particular, it can be observed that the loss coefficient of the outermost jet drops from 0.67 to 0.48 when gap changes from $h = 5$ mm to 1 millimeter. As the impingement surface is moved further away, area increases, and consequently the air pressure decreases. This results in the straightening out of the jet flow.

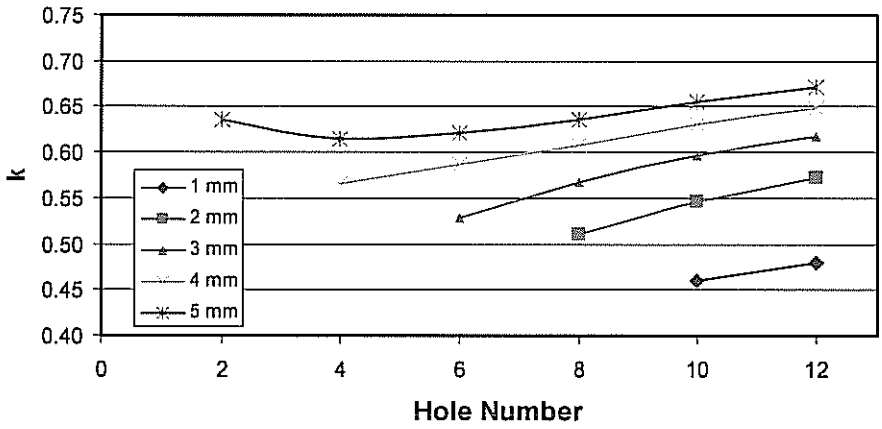


Figure 13 - Loss coefficients for varying hole number.

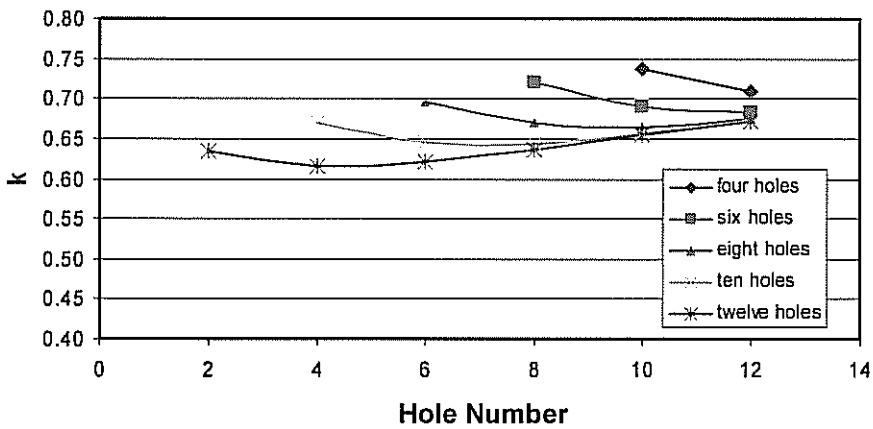


Figure 14 - Loss coefficients of twelve hole largest pitch varying gap heights.

## 7 COMPARISON OF 2D-CFD MODEL AND 1D-AVERAGED RESULTS

The results presented in Section 4 showed that the loss coefficient $\kappa_L$ depends on the clearance $h$, the hole-pitch $S$, and number of holes in a complex manner. In this section, the pressure distributions on the top plate, predicted by the 2D-CFD solution and the 1D-averaged solution given by Equation (5) are compared. This comparison is carried out for twelve-hole configuration with $S = 3$ mm in Figure 15 and $S = 24$ mm in Figure 16, for $h = 1$, 3, and 5 mm. In calculating Figures 15 and 16, $\kappa = 0.65$, $\alpha = 1/3$ and 1/9, and $l =$ 0.36 mm and 0.141 mm, respectively, were used in Equation (5). These figures show that the difference in average pressure along the confinement surface predicted by the 1D-model and that from numerical solution can range from 15 to 40 Pa, depending on the values of hole-pitch $S$ and clearance $h$ for the configuration. The 1D-model gives better predictions when hole pitch is small, as this configuration results in smoother transition of the air pressure between the jets, as mentioned before. On the other hand, prediction

accuracy decreases with increasing hole-pitch, as the sources behave more like individual jets.

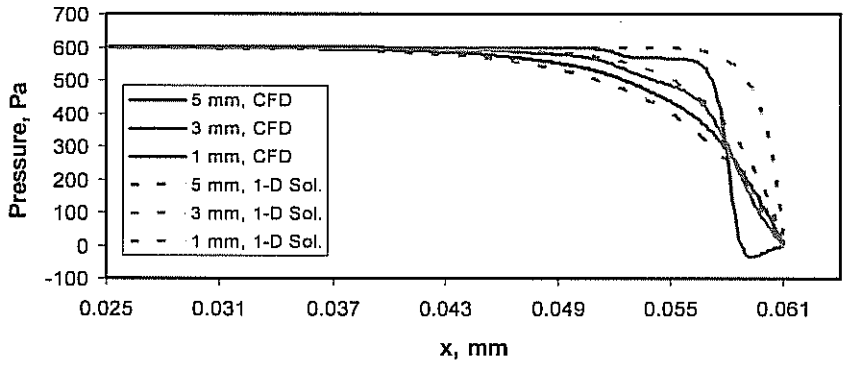


Figure 15 – Pressure profiles of twelve hole smallest pitch varying gap heights.

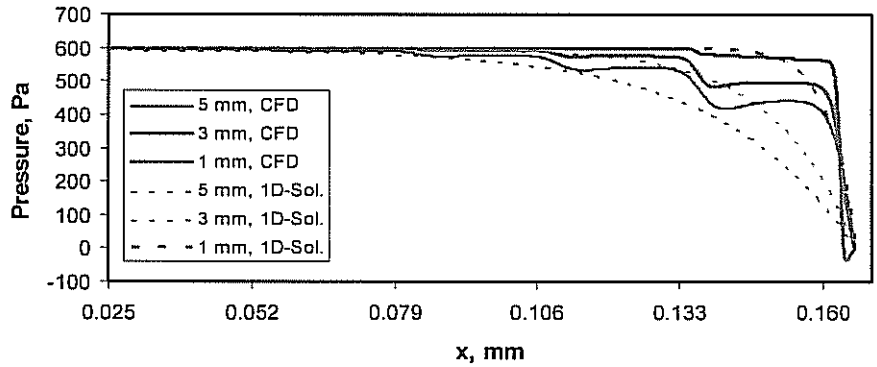


Figure 16 – Pressure profiles of twelve hole largest pitch varying gap heights.

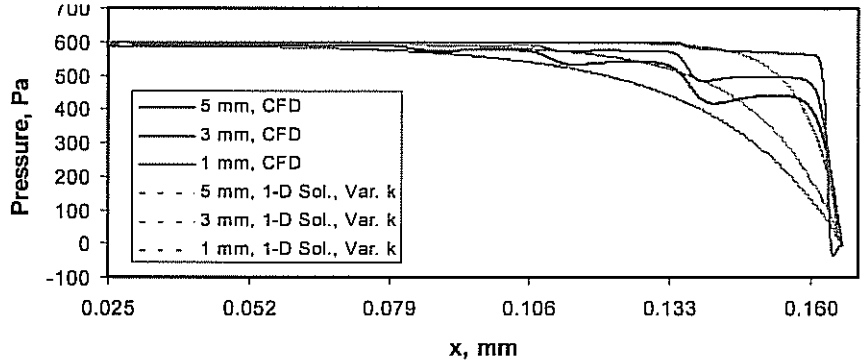


Figure 17 – Pressure profiles of twelve hole smallest pitch with varying gap heights using new loss coefficient model.

To account for losses associated with jet interaction a variable loss coefficient model can be used. A model based on information from Section 6 would increase flow on the outer holes of the reverser by raising the loss coefficient. Such a model has been developed in

reference [17]. Figure 17 shows the comparison of the CFD-solutions with the solution of Equations (1) – (3) with the variable $\kappa_L$ model developed in [17]. This figure shows that using the variable loss coefficient increases the accuracy of the predictions pressure profiles for small hole pitch, reducing the difference in average pressure predictions and numerical values by 5 to 10 Pa. The largest pitch still poses problems due to the increase in jet interaction. Overall the 1D-model using a constant discharge coefficient holds reasonably well for smaller pitch, but fails for large pitch.

## 8 SUMMARY AND CONCLUSIONS

The fluid mechanics of the airflow in the interface of a reverser and a web, which is assumed rigid, is investigated. This type of airflow had been previously modeled as 2D-in the plane of the web ($x$-$y$ plane) [1]. In that original work, the flow-loss around each pressure hole was modeled by a constant discharge coefficient $\kappa$; and, the holes were assumed to be sufficiently close, to allow the use of a distributed hole density $\alpha(x, y)$.

In this paper holes are modeled directly as 2D-infinitely wide slots, and the hole interactions are investigated using the CFD code Fluent (ver. 5.5, Lebanon, New Hampshire) in a plane perpendicular to the reverser surface ($x$-$z$ plane). This provides a dimension of analysis not seen in the 2D flow equations developed before [1]. The flow analyzed by Fluent behaves similar to multiple impinging slot jets with a self-produced cross-flow. In order to understand the physical parameters which affect jet interaction the channel clearance, hole-pitch, number of holes and the supply pressure were investigated.

Five characteristic flow regions were identified the *confined jet exit* region, the *impinging jet* region, the *wall jet* region, the *vortices* region, and the *stalled flow* region. It was shown that the wall jet produced by the exiting jet flow and the vortices created by the trapped flow have strong influence on the jet interactions. It was also shown that:

a) Small channel height forces the wall jet into the neighboring jet, thus creating more interaction and decreasing the size of the vortices.
b) Greater hole-pitch provides the wall jet more space to develop and increase the interaction with the neighboring jet.
c) Top wall pressure in the hole-region, was shown to drop with increasing channel height, as air is allowed to exit more easily.
d) Increasing the hole-pitch caused the air pressure in the hole-region to became less uniform and drop, as in this case each hole acts more as an individual jet.

The loss coefficient was defined as the ratio of the vertical component of the average velocity obtained from the numerical analysis to the ideal exit-hole velocity obtained from Bernoulli's equation. It was shown that:

a) The loss coefficient varies from jet-to-jet.
b) Larger channel height and larger hole-pitch cause more loss (i.e., lower loss coefficient) as more jet interaction is produced.
c) Supply pressure has little effect on the loss coefficient.
d) The jet interaction increases with number of holes, resulting in lower loss coefficient. However, it was also found that a given jet is affected by only two jets located upstream.

When the 1D model [1] is compared to the CFD results, it was found that the use of a variable loss coefficient model did not produce substantial improvements as compared to the to constant $\kappa$ model. However, in general, the 1D model gives a closer approximation to the CFD model for larger values of the channel height and closer hole-spacing configurations.

## REFERENCES


[1] Müftü, S., Lewis, T.S., Cole, K.A. and Benson, R.C., "A Two Dimensional Model of the Fluid Dynamics of an Air Reverser," Journal of Applied Mechanics, Trans. ASME, Vol. 65, No. 1, 1998 ,pp. 171-177.

[2] Al-Sanea, S., "A Numerical Study of the Flow and Heat Transfer Characteristics of an Impinging Laminar Slot Jet Including Cross Flow Effects," International Journal of Heat and Mass Transfer, Vol. 35, 1992, pp. 2501-2513.

[3] Yang, Y. T. and Hao, T. P., "Numerical Studies of Three Turbulent Slot Jets with and without Moving Surface," Acta Mechanica, Vol. 136, 1999, pp. 17-27.

[4] Barata, J. M. M., Durão, D. F. G. and Heitor, M.V., "Velocity Characteristics of Multiple Impinging Jets through a Crossflow," Journal of Fluids Engineering, Vol.114, 1992, pp. 231-239.

[5] Saas, N. R., Polat, S. and Douglas, J. W., "Confined Multiple Impinging Slot Jets Without Crossflow Effects," International Journal of Fluid Flow, V. 13, No. 1, 1992, pp. 2-14.

[6] Kim, S. W. and Benson, T. J., "Fluid Flow of a Row of Jets in Crossflow-A Numerical Study," AAIA Journal, Vol. 31, 1993, pp. 806-811.

[7] Seyedein, S. H., Hassan, M., and Mujumdar, A. S., "Turbulent Flow and Heat Transfer from Confined Multiple Impinging Jets," Numerical Heat Transfer, Vol. 27, 1995, pp. 35-351.

[8] Fluent Ver. 5.5 Users Guide, Fluent Inc., Lebanon, New Hampshire, 2001.

[9] Spalart, P. and Allmaras, S., "A One-Equation Turbulence Model for Aerodynamic Flows," Technical Report AIAA-92-0439, American Institute of Aeronautics and Astronautics, 1992.

[10] Albabbagh, L. B.Y., and Sezai, I., "Numerical Simulation of Three-Dimensional Laminar Multiple Impinging Square Jets," International Journal of Heat and Fluid Flow, Vol. 23, 2002, pp. 509-518.

[11] Aldabbagh, L. B. Y., Sezai, I. and Mohamad, A. A., "Three-Dimensional Investigation of a Laminar Impinging Square Jet Interaction with Cross Flow," Journal of Heat Transfer, Vol. 125, 2003, pp. 243-249.

[12] Theilen, L., Jonker, H. J. J. and Hanjalic, K., "Symmetry Breaking of Flow and Heat Transfer in Multiple Impinging Jets," International Journal of Heat and Fluid Flow, Vol. 24, 2003, pp. 444-453.

[13]Barata, J. M. M., "Fountain Flows Produced by Multiple Impinging Jets in a Crossflow," AIAA Journal, Vol. 34, 1996, pp. 2523-2530.

[14] Aldabbagh, L. B. Y. and Sezai, I., "Numerical Simulation of Three Dimensional Laminar, Square Twin Jet Impingement on a Flate Plate, Flow Structure and Heat Transfer," Numerical Heat Transfer, Vol. 41, 2002, pp. 835-850.

[15] Yang, Y. T. and Shyu, C. H., "Numerical Study of Multiple Impinging Slot Jets with an Inclined Confinement Surface," Numerical Heat Transfer,Vol. 33, 1998, pp. 23-37.

[16] Gerhart, P. M, Gross, R. J. and Hochstein, J. I., Fundamentals of Fluid Mechanics, 2nd ed., Addison-Wesley Publishing Company, New York, 1992, pp.526-527.

[17] Lopez, Ernesto, "Numerical Investigations of Discharge Coefficient for Slot Jets in a Confined Channel with a Self Generated Crossflow," Northeastern University, Boston, MA, 2005.

*Investigation of Fluid Mechanics of Slotted Air-Jets for Air Reverser Applications*

**E. Lopez & S. Müftü,**
Northeastern University,
USA

| **Name & Affiliation** | **Question** |
|---|---|
| Herong Lei<br>Eastman Kodak | The plate on the top is kind of stationary, right? If you think about on a machine the web is moving at 300 m/min. Will that impact your results? |
| **Name & Affiliation** | **Answer** |
| Ernesto Lopez<br>Northeastern University | Due to shear at the wall we assume that the flow will now have a flow pattern towards one side of the configurations. We wouldn't be able to assume this symmetry that we took into account at the beginning and right now we're just trying to look at the flow regions without the moving web. |
| **Name & Affiliation** | **Question** |
| Jan-Erik Olsen<br>SINTEF | In this analysis you assume a gap. I believe in Fluent you could also do a calculation and calculate the gap. If that turns out too difficult you could also probably simulate it with a web tension which is in equilibrium with pressure on the web surface. Have you considered this? |
| **Name & Affiliation** | **Answer** |
| Ernesto Lopez<br>Northeastern University | The plan is to take my part, the CFD modeling by and combine it with the work of another master student who is taking the profile of the web due to the pressure profile along the web. It is a two part problem. |